

A spin-cell for spin current

Qing-feng Sun¹, Hong Guo¹, and Jian Wang²

¹*Center for the Physics of Materials and Department of Physics, McGill University, Montreal, PQ, Canada H3A 2T8.*

²*Department of Physics, The University of Hong Kong, Pokfulam Road, Hong Kong, China*

Abstract

We propose and investigate a spin-cell device which provides the necessary spin-motive force to drive a spin current for future spintronic circuits. Our spin-cell have four basic characteristics: (i) it has two poles so that a spin current flows in from one pole and out from the other pole, this way a complete spin-circuit can be established; (ii) it has a source of energy to drive the spin current; (iii) it maintains spin coherence so that a sizable spin current can be delivered; (iv) it drives a spin current without a charge current. The proposed spin-cell for spin current should be realizable using technologies presently available.

85.35.-p, 73.23.-b, 72.25.Pn, 73.40.Gk

Traditional electronics is based on the flow of charge: the spin of electron is ignored. The emerging technology of spintronics will make the leap such that the flow of spin—in addition to charge, will be used for electronic applications [1,2]. A spin current is produced by the motion of spin-polarized electrons, therefore spin current is typically associated with spin-polarized charge current [1]. Nevertheless, if one can generate an ideal situation as shown in Fig.(1a) where spin-up electrons move to the right while an equal number of spin-down electrons move to the left, then there will be no net charge current because $I_e \equiv e(I_{\uparrow} + I_{\downarrow}) = 0$ where eI_{\uparrow} , eI_{\downarrow} are charge currents due to spin-up and spin-down electrons, respectively. There will be, however, a finite spin current: $I_s \equiv \frac{\hbar}{2}(I_{\uparrow} - I_{\downarrow})$ where \hbar is the reduced Planck constant. Considering the interesting and important future perspective of spin-current circuit, it is crucial to have a spin-cell that satisfies the four characteristics discussed in the Abstract and it produces the flow pattern of Fig.(1a) [3]. In this paper we theoretically propose and analyze such a spin-cell.

Our spin-cell is schematically shown in Fig.(1b). It consists of a double quantum-dot (QD) fabricated in two-dimensional electron gas (2DEG) with split gate technology, and each QD is contacted by an electrode. Note that no magnetic material is involved. The two QDs and their associated contacts to the electrodes serve as the “positive/negative” poles of the spin-cell. The two electrodes maintain the same electrochemical potential $\mu_L = \mu_R$ (*i.e.* no bias voltage is applied on them). The size of the spin-cell structure is assumed to be within the spin coherence length which can be as long as many microns for 2DEG. We control the QD energy levels by gate voltages $V_{g\alpha}$ where $\alpha = L, R$ indicates the left/right QD. Both QD levels are controlled by an overall gate voltage V_g , see gate arrangements in Fig.(1b). In order to distinguish spin-up electrons from spin-down electrons, a spatially *non-uniform* external magnetic field B_{α} is applied to the two QDs—perpendicular to the QD plane. An extreme case of non-uniformity is $B_R = -B_L$, *i.e.* equal in value but opposite in direction. This particular magnetic field distribution is not necessary at all for the operation of our spin-cell, but it helps us to discuss its physics. Finally, the energy source of our spin-cell is provided by shining a microwave radiation with strengths Δ_L/Δ_R for the left/right

QDs. Because, typically, the microwave frequency is far less than the plasma frequency of the material covering the QDs, the effect of the microwave field is to induce a high frequency potential variation $\Delta_{L/R} \cos \omega t$ in the left/right QD and their leads. [4] When $\Delta_L \neq \Delta_R$, a time-dependent potential difference, $\Delta \cos \omega t = (\Delta_L - \Delta_R) \cos \omega t$, exists between the two QDs. An a.c. electric field $\mathbf{E}(t)$ in the middle barrier is therefore established due to the microwave radiation (see Fig.(1c)). Then, electrons can absorb photons when they pass the middle barrier of the device. The establishment of $\mathbf{E}(t)$ across the two QDs is necessary for our spin-cell to work, here we use a non-uniform microwave radiation to achieve this effect as has already been carried out experimentally [5], but other possibilities also exist.

Before we present theoretical and numerical results of the device in Fig.(1b), we first discuss why it works as a spin-cell. The physics is summarized in Fig.(1c). To be specific, let B_R point to $-z$ direction and B_L to $+z$ direction. Due to Zeeman effect, a spin-degenerate level ϵ_R on the right QD is now split into spin-down/up levels $\epsilon_{R\downarrow} < \epsilon_{R\uparrow}$. On the left QD, it is $\epsilon_{L\uparrow} < \epsilon_{L\downarrow}$. Electrons in the electrodes can now tunnel into the QD: on the right a spin-down electron is easier to tunnel because level $\epsilon_{R\downarrow}$ is lower, while a spin-up electron is easier to tunnel into the left QD. Once levels $\epsilon_{R\downarrow}, \epsilon_{L\uparrow}$ are occupied, the charging energies U_R, U_L of the two QDs push the other two levels $\epsilon_{R\uparrow}, \epsilon_{L\downarrow}$ to higher energies $\epsilon_{R\uparrow} + U_R, \epsilon_{L\downarrow} + U_L$, and the energy level positions indicated by the solid horizontal lines of Fig.(1c) are established. Next, the spin-down electron on the right QD can absorb a photon and make a transition to the level at $\epsilon_{L\downarrow} + U_L$ on the left QD: afterwards it easily flows out to the left electrode because $\epsilon_{L\downarrow} + U_L > \mu_L$. This process is indicated as $A-$. Similarly the spin-up electron on the left QD flows out to the right electrode after absorption of a photon, indicated by $A+$. This way, driven by the potential variations of the QD induced by the microwave field, a spin-down electron flows to the left while a spin-up electron flows to the right of the spin-cell, and the continuation of the $A-, A+$ processes generates a DC spin current that flows from the left electrode, through the spin-cell, and out to the right electrode. Clearly, if the two processes are absolutely equivalent, there will be no charge current and only a spin current. Finally, since the spin-motive force is provided by a time-dependent change of the electronic

potential landscape of the QD, there is no spin flip mechanism and the spin current flowing through the spin-cell is conserved, *i.e.* $I_{s,L} = -I_{s,R} = I_s$. Our device then satisfies the four characteristics of a spin-cell discussed in the Abstract.

The last paragraph discusses the operation principle of the spin-cell for spin current, but there are other interesting device details which can only be obtained by detailed theoretical and numerical analysis for which we now turn. The spin-cell of Fig.(1b) is described by the following Hamiltonian: [4,6]

$$\begin{aligned}
H = & \sum_{\alpha\sigma} [\epsilon_\alpha + W_\alpha(t) - (1/2)\sigma g\mu B_\alpha] d_{\alpha\sigma}^\dagger d_{\alpha\sigma} \\
& + \sum_{\alpha} U_\alpha d_{\alpha\uparrow}^\dagger d_{\alpha\uparrow} d_{\alpha\downarrow}^\dagger d_{\alpha\downarrow} + \sum_{k\sigma\alpha} [\epsilon_{\alpha k} + W_\alpha(t)] a_{\alpha k\sigma}^\dagger a_{\alpha k\sigma} \\
& + \sum_{k\sigma\alpha} [t_{\alpha k} a_{\alpha k\sigma}^\dagger d_{\alpha\sigma} + H.c.] + \sum_{\sigma} [t_C d_{L\sigma}^\dagger d_{R\sigma} + H.c.] \quad (1)
\end{aligned}$$

where $a_{\alpha k\sigma}^\dagger$ ($a_{\alpha k\sigma}$) and $d_{\alpha\sigma}^\dagger$ ($d_{\alpha\sigma}$) are creation (annihilation) operators in the electrode α and the dot α , respectively. The left and right QD includes a single energy level ϵ_α , but has spin index σ and intradot Coulomb interaction U_α . To account for the magnetic field B , the left/right QD's single particle energy has a term $-(1/2)\sigma g\mu B_\alpha$, in which we have required a different magnetic field strength for the two QDs, *i.e.* $B_L \neq B_R$. t_C and $\Gamma_\alpha \equiv 2\pi \sum_k |t_{\alpha k}|^2 \delta(\epsilon - \epsilon_{\alpha k})$ describe the coupling strength between the two QDs, and between electrode α and its corresponding QD, respectively. The microwave irradiation is given by [4,6] $W_\alpha(t) = \Delta_\alpha \cos\omega t$ and it produces an adiabatic change for the single particle energy. Here we permit the microwave field to irradiate the entire device including the electrodes, and we require a difference in the radiation strength $\Delta_L \neq \Delta_R$.

Our theoretical analysis of the spin-cell is based on standard Keldysh nonequilibrium Green's function (NEGF) theory [4,6] which we briefly outline here. First, we perform an unitary transformation of the Hamiltonian with an unitary operator $U(t) = \exp\left\{i \int_0^t dt' \sum_{\alpha} W_\alpha(t') \hat{D}\right\}$, where $\hat{D} \equiv \sum_{k\sigma} a_{\alpha k\sigma}^\dagger a_{\alpha k\sigma} + \sum_{\sigma} d_{\alpha\sigma}^\dagger d_{\alpha\sigma}$. The Hamiltonian H is transformed to the following form,

$$H = \sum_{\alpha\sigma} [\epsilon_\alpha - \sigma g\mu B_\alpha/2] d_{\alpha\sigma}^\dagger d_{\alpha\sigma} + \sum_{\alpha} U_\alpha d_{\alpha\uparrow}^\dagger d_{\alpha\uparrow} d_{\alpha\downarrow}^\dagger d_{\alpha\downarrow}$$

$$\begin{aligned}
& + \sum_{k\sigma\alpha} \epsilon_{\alpha k} a_{\alpha k\sigma}^\dagger a_{\alpha k\sigma} + \sum_{k\sigma\alpha} \left[t_{\alpha k} a_{\alpha k\sigma}^\dagger d_{\alpha\sigma} + H.c. \right] \\
& + \sum_{\sigma} \left[t_C e^{i \int_0^t dt' \Delta \cos \omega t'} d_{L\sigma}^\dagger d_{R\sigma} + H.c. \right], \tag{2}
\end{aligned}$$

where $\Delta \equiv \Delta_L - \Delta_R$. In (2), we take the last term which explicitly depends on time t as the interacting part H_I , and the remaining part as $H_o \equiv H - H_I$. The Green's function of H_o , $g^r(\epsilon)$, can be easily obtained with a decoupling approximation at the Hartree level [7],

$$g_{\alpha\alpha\sigma}^r(\epsilon) = \frac{\epsilon_{\alpha\sigma}^- + U_\alpha n_{\alpha\bar{\sigma}}}{(\epsilon - \epsilon_{\alpha\sigma})\epsilon_{\alpha\sigma}^- + \frac{i}{2}\Gamma_\alpha(\epsilon_{\alpha\sigma}^- + U_\alpha n_{\alpha\bar{\sigma}})}, \tag{3}$$

where $\epsilon_{\alpha\sigma}^- \equiv \epsilon - \epsilon_{\alpha\sigma} - U_\alpha$, $\epsilon_{\alpha\sigma} \equiv \epsilon_\alpha - \sigma g \mu B_\alpha / 2$, and $n_{\alpha\bar{\sigma}}$ is the time-averaged intradot electron occupation number at the state $\bar{\sigma}$ in the α -QD which we solve self-consistently. It is worth mentioning that $g_{\alpha\alpha\sigma}^r(\epsilon)$ in Eq.(3) has two resonances: one is at $\epsilon_{\alpha\sigma}$ while its associated state at $\epsilon_{\alpha\bar{\sigma}}$ is empty; the other resonance is at $\epsilon_{\alpha\sigma} + U_\alpha$ while its associated state $\epsilon_{\alpha\bar{\sigma}}$ is occupied. Notice, in H_o the left part of the spin-cell (*i.e.* the left-lead and the left-QD) is not coupled with the right part of the spin-cell, therefore they are in equilibrium respectively. Hence the Keldysh Green's function $g_{\alpha\alpha\sigma}^<(\epsilon)$ for H_o can be solved from the fluctuation-dissipation theorem: $g_{\alpha\alpha\sigma}^<(\epsilon) = -f_\alpha [g_{\alpha\alpha\sigma}^r(\epsilon) - g_{\alpha\alpha\sigma}^a(\epsilon)]$. With these preparations, the Green's function G^r and $G^<$ of the total Hamiltonian H can be solved. In particular, we calculate $G_{\alpha\beta\sigma}^r(t, t') \equiv -i\theta(t - t') < \{d_{\alpha\sigma}(t), d_{\beta\sigma}^\dagger(t')\} >$ by iterating the Dyson equation. In Fourier space, the Dyson equation can be reduced to [8,9]

$$\mathbf{G}_{\sigma;mn}^r(\epsilon) = \mathbf{g}_{\sigma;mn}^r(\epsilon) + \sum_k \mathbf{G}_{\sigma;mk}^r(\epsilon) \Sigma_{\sigma;kn}^r(\epsilon) \mathbf{g}_{\sigma;nm}^r(\epsilon),$$

where $\mathbf{G}_{\sigma;mn}^r(\epsilon) \equiv \mathbf{G}_{\sigma,n-m}^r(\epsilon + m\omega)$, and the quantity $G_n(\epsilon)$ is the Fourier expansion of $G(t, t')$. [8] The retarded self-energy $\Sigma_{\sigma;kn}^r(\epsilon)$ is the Fourier transform of $\Sigma_\sigma^r(t_1, t_2)$ where $\Sigma_{LR\sigma}^r(t_1, t_2) = \Sigma_{RL\sigma}^{r*}(t_1, t_2) = \delta(t_1 - t_2) t_C \exp[i \int_0^{t_1} dt' \Delta \cos \omega t']$, and $\Sigma_{LL\sigma}^r = \Sigma_{RR\sigma}^r = 0$. We obtain $\Sigma_{LR\sigma, mn}^r(\epsilon) = \Sigma_{RL\sigma, nm}^{r*}(\epsilon) = t_C J_{n-m}(\frac{\Delta}{\omega})$. The Green's function $\mathbf{g}_{\sigma;mn}^r(\epsilon)$ is: $g_{\alpha\beta\sigma;mn}^r(\epsilon) = \delta_{\alpha\beta} \delta_{mn} g_{\alpha\alpha\sigma}^r(\epsilon + m\omega)$. Then $\mathbf{G}_{\sigma;mn}^r(\epsilon)$ can be solved from the above Dyson equation: [10]

$$G_{\alpha\alpha\sigma, mn}^r(\epsilon) = \delta_{mn} / \left[\left(g_{\alpha\alpha\sigma, mm}^r \right)^{-1} - A_{\bar{\alpha}\sigma, mm} \right],$$

$$G_{\alpha\bar{\alpha}\sigma,mm}^r(\epsilon) = G_{\alpha\alpha\sigma,mm}^r(\epsilon)\Sigma_{\alpha\bar{\alpha}\sigma,mm}^r g_{\alpha\bar{\alpha}\sigma,nn}^r(\epsilon),$$

where $A_{\alpha\sigma,mm}(\epsilon) \equiv \sum_k |t_C|^2 J_{k-m}^2 \left(\frac{\Delta}{\omega}\right) g_{\alpha\alpha\sigma;kk}^r(\epsilon)$. Afterwards, the total Keldysh Green's function $G_{\alpha\beta\sigma}^<(t, t') \equiv i \langle d_{\beta\sigma}^\dagger(t') d_{\alpha\sigma}(t) \rangle$ is easily obtained from the Keldysh equation. Finally, we obtain the time-averaged current in lead α from

$$I_{\alpha\sigma} \equiv \langle I_{\alpha\sigma}(t) \rangle = -Im \int (d\epsilon/2\pi) \Gamma_\alpha(\epsilon) \left[G_{\alpha\alpha\sigma,00}^<(\epsilon) + 2f_\alpha(\epsilon) G_{\alpha\alpha\sigma,00}^r(\epsilon) \right], \quad (4)$$

and the self-consistent equation for the intradot occupation number $n_{\alpha\sigma}$: $n_{\alpha\sigma} = -i \int (d\epsilon/2\pi) G_{\alpha\alpha\sigma,00}^<(\epsilon)$.

Fig.(2) shows the calculated charge current I_e (in units of e) and the spin current I_s (units of $\hbar/2$) versus the gate voltage V_{gR} at different microwave frequency ω . I_e shows a positive peak due to the $A+$ process and a negative peak by the $A-$ process (see Fig.(1c)), but I_s has two positive peaks. As we tune the gate voltage V_{gR} , the right QD level is shifted so that when $\hbar\omega = \epsilon_{L\downarrow} + U_L - \epsilon_{R\downarrow}$, the $A-$ process occurs with high probability leading to a positive peak in I_s and a negative peak in I_e . On the other hand we get positive peaks in both I_e and I_s when $\hbar\omega = \epsilon_{R\uparrow} + U_R - \epsilon_{L\uparrow}$, for the the $A+$ process.

The peak positions in I_e, I_s due to the $A\pm$ processes shift linearly with the microwave frequency ω , as shown by the dotted lines in Fig.(2). Eventually, at a special frequency indicated by A , *i.e.* when $\hbar\omega^* = \epsilon_{R\uparrow} + U_R - \epsilon_{L\uparrow} = \epsilon_{L\downarrow} + U_L - \epsilon_{R\downarrow}$, the two peaks overlap so that the net charge current I_e cancels exactly due to the cancellation of the $A\pm$ processes, at the same time the spin current I_s doubles its value. At this special frequency, the full operation of the spin-cell occurs so that a spin current is driven across the spin-cell, from left electrode to the right electrode, without a charge current. If we connect the spin-cell to complete an external circuit, a spin current will be driven and continue to flow across the spin-cell into the circuit. [11] On the other hand, if we let the two poles of the spin-cell open, although I_s must be zero, a spin-motive force in the two poles of the spin cell will still be induced so that chemical potential $\mu_{\alpha\uparrow} \neq \mu_{\alpha\downarrow}$. For example, in the case of Fig.(1c), an open circuit will lead to $\mu_{L\uparrow} < \mu_{L\downarrow}$ and $\mu_{R\uparrow} > \mu_{R\downarrow}$.

In the following we focus on the spin-cell operation by fixing gate voltage $V_{gR} = 0.45$ which is its value at point A of Fig.(2). We investigate I_e, I_s as functions of the overall gate potential V_g (Fig.(3a)), magnetic field $g\mu B_L$ (Fig.(3b)), and frequency ω (Fig.(3c)). Different curves in Fig.(3) correspond to different microwave strength $\Delta \equiv \Delta_L - \Delta_R$. In all situations $I_e \approx 0$ and we do not discuss it anymore. Fig.(3c) shows that I_s has several peaks and dips when we vary ω : the large peak indicated by A is the spin-cell operation discussed above, but peaks at C and D correspond to double- and triple-photon processes which connect the $A\pm$ transitions of Fig.(1c). The dip at B originates from less probable transitions connecting levels indicated by the dashed lines of Fig.(1c), while the dip at E is its two-photon process. Now, fixing ω at ω^* , *i.e.* at the spin-cell operation point A, the value of I_s can be tuned by the overall gate voltage V_g as shown in Fig.(3a). However, I_s keeps large values for a wide range of V_g : this range is in the Coulomb interaction scale $U/e!$ This is important, because in an experimental situation any background charge or environmental effect near the spin-cell may alter the overall potential, and Fig.(3a) shows that the spin-cell operation is not critically altered by this effect. When V_g becomes very large so that $\epsilon_{L\downarrow} + U_L$ and $\epsilon_{R\uparrow} + U_R$ is below the chemical potential μ , or $\epsilon_{L\uparrow}$ and $\epsilon_{R\downarrow}$ is above μ , I_s diminishes because the $A\pm$ processes can no longer occur (see Fig.(1c)). Finally, a very important result is shown in Fig.(3b), where we fixed $g\mu B_R = -0.4$ while varying $g\mu B_L$ at the spin-cell operation point [12] A . Fig.(3b) shows clearly that I_s increases with an increasing difference of $(B_L - B_R)$: $I_s = 0$ identically when $B_L = B_R$ if $U_L = U_R$, or $I_s \approx 0$ if $U_L \neq U_R$. However, Fig.(3b) demonstrates that we only need a slight difference in B_L and B_R , at a scale of the coupling constant Γ_α , to generate a substantial I_s . The most important fact is that B_L and B_R do not have to point to opposite directions which is experimentally difficult to do. In fact, if the two QD's are fabricated with different materials so that the g -factors are different, one can actually use an *uniform* magnetic field throughout.

The proposed spin-cell for spin current should be experimentally feasible using present technologies. First, the double-QD structures can and have been fabricated by several laboratories. Second, microwave assisted quantum transport measurements have recently

been reported [5,13,14]. In particular, the asymmetrical microwave radiation on double-QD device (**i.e.** $\Delta_L \neq \Delta_R$) has already been carried out experimentally [5]. Third, the asymmetric magnetic field should be feasible as we have discussed above. If one takes $f = \omega/2\pi = 50\text{GHz}$, arranges the corresponding $U(\sim \hbar\omega) \approx 0.2\text{meV}$, and fixes the temperature scale $K_B T$ and coupling Γ_α to be twenty times less than U as in typical QD experiments, *i.e.* $k_B T = 100\text{mK}$ and $\Gamma = 10\mu\text{eV}$, the corresponding magnetic field difference is $(g\mu(B_L - B_R) \sim \Gamma) |B_L - B_R| \sim 0.16/g$ tesla. These QD parameters have already been realized by present technology. Finally, it is not difficult to show that by adjusting the gate voltages one can easily calibrate the spin-cell operating point [15].

Acknowledgments: We gratefully acknowledge financial support from NSERC of Canada, FCAR of Quebec (Q.S., H.G), and a RGC grant from the SAR Government of Hong Kong under grant number HKU 7091/01P (J.W.). H.G. thanks Dr. Junren Shi for a discussion on photon assisted tunneling. We gratefully acknowledge Dr. Baigeng Wang for many discussions and inputs on the physics of spin current.

Appendix A

In this appendix, we give a detailed derivation process of the unitary transformation in which the Hamiltonian (1) is transformed to Hamiltonian (2) in the manuscript. We take the unitary matrix $U(t)$ as:

$$U(t) = \exp \left\{ i \int_0^t dt' \sum_{\alpha} \left[W_{\alpha}(t') \left(\sum_{k\sigma} a_{\alpha k\sigma}^{\dagger} a_{\alpha k\sigma} + \sum_{\sigma} d_{\alpha\sigma}^{\dagger} d_{\alpha\sigma} \right) \right] \right\} \quad (A1)$$

Under this unitary transformation, the operator X_{α} (X_{α} represents $a_{\alpha k\sigma}$ and $d_{\alpha\sigma}$) and X_{α}^{\dagger} transform into:

$$U(t)X_{\alpha}U^{\dagger}(t) = X_{\alpha}\exp \left[-i \int_0^t dt' W_{\alpha}(t') \right] \quad (A2)$$

$$U(t)X_{\alpha}^{\dagger}U^{\dagger}(t) = X_{\alpha}^{\dagger}\exp \left[i \int_0^t dt' W_{\alpha}(t') \right] \quad (A3)$$

Because unitary matrix $U(t)$ is dependent of time t , the Hamiltonian H after the unitary transformation is:

$$H_{new}(t) = U(t)H(t)U^{\dagger}(t) - U(t)i\frac{\partial}{\partial t}U^{\dagger}(t) \quad (A4)$$

Using Eqs.(A2) and (A3), we easily obtain the new Hamiltonian (2) as given in the manuscript. We emphasize that this transform is done exactly and no approximation is involved.

Appendix B

In this Appendix, we present a detailed derivation for the retarded Green's function $g_{\alpha\alpha\sigma}^r(\epsilon)$ (Eq.(3) in the manuscript) of the Hamiltonian H_0 . Here, we solve $g_{\alpha\alpha\sigma}^r(\epsilon)$ by using the equation of motion method:

$$\epsilon \ll \hat{A}|\hat{B} \gg^r = \langle \{\hat{A}, \hat{B}\} \rangle + \ll [\hat{A}, H_0]|\hat{B} \gg^r \quad (B1)$$

where \hat{A} and \hat{B} represent arbitrary operators, and $\ll \hat{A}|\hat{B} \gg^r$ is the Fourier expansion of the retarded Green's function $-i\theta(t) \langle \{\hat{A}(t), \hat{B}(0)\} \rangle$. Because H_0 is independent of time t , $\ll \hat{A}(t)|\hat{B}(t') \gg^r$ only depends on the time difference $t - t'$. Applying equation of motion to the Green function $g_{\alpha\alpha\sigma}^r = \ll d_{\alpha\sigma}|d_{\alpha\sigma}^\dagger \gg^r$, we have:

$$(\epsilon - \epsilon_{\alpha\sigma}) \ll d_{\alpha\sigma}|d_{\alpha\sigma}^\dagger \gg^r = 1 + \sum_k t_{k\alpha}^* \ll a_{\alpha k\sigma}|d_{\alpha\sigma}^\dagger \gg^r + U_\alpha \ll d_{\alpha\sigma}d_{\alpha\bar{\sigma}}^\dagger d_{\alpha\bar{\sigma}}|d_{\alpha\sigma}^\dagger \gg^r \quad (B2)$$

and

$$\ll a_{\alpha k\sigma}|d_{\alpha\sigma}^\dagger \gg^r = \frac{t_{k\alpha}}{\epsilon - \epsilon_{k\sigma} + i0^+} \ll d_{\alpha\sigma}|d_{\alpha\sigma}^\dagger \gg^r \quad (B3)$$

Substitute Eq.(B3) into Eq.(B2), we obtain:

$$(\epsilon - \epsilon_{\alpha\sigma} - \Sigma_\alpha^r) \ll d_{\alpha\sigma}|d_{\alpha\sigma}^\dagger \gg^r = 1 + U_\alpha \ll d_{\alpha\sigma}d_{\alpha\bar{\sigma}}^\dagger d_{\alpha\bar{\sigma}}|d_{\alpha\sigma}^\dagger \gg^r \quad (B4)$$

where $\Sigma_\alpha^r \equiv \sum_k \frac{|t_{k\alpha}|^2}{\epsilon - \epsilon_{k\sigma} + i0^+} = \frac{-i}{2}\Gamma_\alpha$ is the self-energy function.

At this point, if one takes a decoupling approximation for the new Green's function $\ll d_{\alpha\sigma}d_{\alpha\bar{\sigma}}^\dagger d_{\alpha\bar{\sigma}}|d_{\alpha\sigma}^\dagger \gg^r$ in Eq.(B4), *i.e.*,

$$\ll d_{\alpha\sigma}d_{\alpha\bar{\sigma}}^\dagger d_{\alpha\bar{\sigma}}|d_{\alpha\sigma}^\dagger \gg^r = n_{\alpha\bar{\sigma}} \ll d_{\alpha\sigma}|d_{\alpha\sigma}^\dagger \gg^r \quad (B5)$$

This is the mean field approximation.

Rather, we continue apply the equation of motion to $\ll d_{\alpha\sigma} d_{\alpha\bar{\sigma}}^\dagger |d_{\alpha\sigma}^\dagger \gg^r$, and we have:

$$\begin{aligned}
(\epsilon - \epsilon_{\alpha\sigma} - U) \ll d_{\alpha\sigma} d_{\alpha\bar{\sigma}}^\dagger |d_{\alpha\sigma}^\dagger \gg^r &= n_{\alpha\bar{\sigma}} \\
&+ \sum_k t_{\alpha k}^* \ll a_{\alpha k\sigma} d_{\alpha\bar{\sigma}}^\dagger |d_{\alpha\sigma}^\dagger \gg^r \\
&- \sum_k t_{\alpha k} \ll d_{\alpha\sigma} a_{\alpha k\bar{\sigma}}^\dagger |d_{\alpha\sigma}^\dagger \gg^r \\
&+ \sum_k t_{\alpha k}^* \ll d_{\alpha\sigma} d_{\alpha\bar{\sigma}}^\dagger a_{\alpha k\bar{\sigma}} |d_{\alpha\sigma}^\dagger \gg^r
\end{aligned} \tag{B6}$$

In this equation, three new Green's functions $\ll a_{\alpha k\sigma} d_{\alpha\bar{\sigma}}^\dagger |d_{\alpha\sigma}^\dagger \gg^r$, $\ll d_{\alpha\sigma} a_{\alpha k\bar{\sigma}}^\dagger |d_{\alpha\sigma}^\dagger \gg^r$, and $\ll d_{\alpha\sigma} d_{\alpha\bar{\sigma}}^\dagger a_{\alpha k\bar{\sigma}} |d_{\alpha\sigma}^\dagger \gg^r$, emerge. We now take the decoupling approximation:

$$\begin{aligned}
\ll a_{\alpha k\sigma} d_{\alpha\bar{\sigma}}^\dagger |d_{\alpha\sigma}^\dagger \gg^r &= n_{\alpha\bar{\sigma}} \ll a_{\alpha k\sigma} |d_{\alpha\sigma}^\dagger \gg^r \\
\ll d_{\alpha\sigma} a_{\alpha k\bar{\sigma}}^\dagger |d_{\alpha\sigma}^\dagger \gg^r &= \ll d_{\alpha\sigma} d_{\alpha\bar{\sigma}}^\dagger a_{\alpha k\bar{\sigma}} |d_{\alpha\sigma}^\dagger \gg^r = 0
\end{aligned} \tag{B7}$$

Eq.(B6) reduces into:

$$(\epsilon - \epsilon_{\alpha\sigma} - U) \ll d_{\alpha\sigma} d_{\alpha\bar{\sigma}}^\dagger |d_{\alpha\sigma}^\dagger \gg^r = n_{\alpha\bar{\sigma}} + \Sigma_\alpha n_{\alpha\bar{\sigma}} \ll d_{\alpha\sigma} |d_{\alpha\sigma}^\dagger \gg^r \tag{B8}$$

Then from Eqs.(B4) and (B8), we can solve the Green's function $g_{\alpha\alpha\sigma}^r(\epsilon) = \ll d_{\alpha\sigma} |d_{\alpha\sigma}^\dagger \gg^r$ as:

$$g_{\alpha\alpha\sigma}^r(\epsilon) = \frac{\epsilon_{\alpha\sigma}^- + U_\alpha n_{\alpha\bar{\sigma}}}{(\epsilon - \epsilon_{\alpha\sigma})\epsilon_{\alpha\sigma}^- - \Sigma_\alpha^r(\epsilon_{\alpha\sigma}^- + U_\alpha n_{\alpha\bar{\sigma}})} \tag{B9}$$

This is the Eq.(3) in the manuscript.

If one applies the equation of motion one more time, on the three new Green's functions of Eq.(B6), then takes a decoupling approximation, the Green function is obtained to be:

$$g_{\alpha\alpha\sigma}^r(\epsilon) = \frac{1 + U_\alpha A_{\alpha\sigma} n_{\alpha\bar{\sigma}}}{\epsilon - \epsilon_{\alpha\sigma} + \frac{i}{2}\Gamma_\alpha + U_\alpha A_{\alpha\sigma} (\Sigma_{\alpha\bar{\sigma}}^{(a)} + \Sigma_{\alpha\bar{\sigma}}^{(b)})} \tag{B10}$$

where the definition of $A_{\alpha\sigma}$, $\Sigma_{\alpha\bar{\sigma}}^{(a)}$ and $\Sigma_{\alpha\bar{\sigma}}^{(b)}$, are given in Phys. Rev. B 64,153306 (2001).

This solution has a Kondo resonance and it has been applied in some previous work for investigating the Kondo effect.

Appendix C

In this Appendix, we give a detailed derivation for the Green's function $G_{\alpha\beta\sigma, mn}^r(\epsilon)$ of the Hamiltonian H . First, from the Dyson equation, we have:

$$G_{LL\sigma, mn}^r = g_{LL\sigma, mn}^r + \sum_k G_{LR\sigma, mk}^r \Sigma_{RL\sigma, kn}^r g_{LL\sigma, nn}^r \quad (C1)$$

$$G_{LR\sigma, mn}^r = \sum_k G_{LL\sigma, mk}^r \Sigma_{LR\sigma, kn}^r g_{RR\sigma, nn}^r \quad (C2)$$

where we have suppressed the argument ϵ . Substitute Eq.(C2) into Eq.(C1), we obtain:

$$G_{LL\sigma, mn}^r = g_{LL\sigma, mn}^r + \sum_{k_1, k_2} G_{LL\sigma, mk_1}^r \Sigma_{LR\sigma, k_1 k_2}^r g_{RR\sigma, k_2 k_2}^r \Sigma_{RL\sigma, k_2 n}^r g_{LL\sigma, nn}^r \quad (C3)$$

Introducing notation $A_{R\sigma, mn}(\epsilon)$,

$$A_{R\sigma, mn}(\epsilon) \equiv \sum_k \Sigma_{LR\sigma, mk}^r g_{RR\sigma, kk}^r \Sigma_{RL\sigma, kn}^r \quad (C4)$$

then the Eq.(C3) reduces to:

$$\begin{aligned} G_{LL\sigma, mn}^r &= g_{LL\sigma, mn}^r + \sum_{k_1} G_{LL\sigma, mk_1}^r A_{R\sigma, k_1 n} g_{LL\sigma, nn}^r \\ &= g_{LL\sigma, mn}^r + \sum_{k_1} g_{LL\sigma, mk_1}^r A_{R\sigma, k_1 n} g_{LL\sigma, nn}^r \\ &+ \sum_{k_1 k_2} g_{LL\sigma, mk_1}^r A_{R\sigma, k_1 k_2} g_{LL\sigma, k_2 k_2}^r A_{R\sigma, k_2 n} g_{LL\sigma, nn}^r + \dots \end{aligned} \quad (C5)$$

In the following we take an approximation as our previous work [Eq.(29) in Phys. Rev B 59,13126 (1999)]:

$$A_{R\sigma, k_1 n} g_{LL\sigma, k_1 k_1}^r g_{LL\sigma, nn}^r = A_{R\sigma, k_1 n} \delta_{k_1 n} \left[g_{LL\sigma, nn}^r \right]^2 \quad (C6)$$

This approximation is reasonable when $\hbar\omega \gg \max(\Gamma_\alpha, t_C)$. In the following we discuss the physical picture of this approximation. The Green's function $G_{LL\sigma, mn}^r$ is a propagator (of the Hamiltonian H) for an electron from the left dot to the left dot. The first term $g_{LL\sigma, mn}^r$ describes that the electron always stays in the left dot. The second term $\sum_{k_1} g_{LL\sigma, mk_1}^r A_{R\sigma, k_1 n} g_{LL\sigma, nn}^r$ describes the propagation process in which the electron from left dot transits to the right dot while absorbing $k_1 - k$ photons, it then stays in the right dot

for some time, then goes back to the left dot emitting $n - k$ photons. The higher order term describes multi-time transit processes between the left dot and the right dot. In our approximation (*e.g.* for the 2nd term), we take $k_1 = n$ and neglect others. We emphasize that this term is indeed the most important. For example, if $k_1 \neq n$, we consider an initial electron in the left dot sitting at the resonance state (*e.g.* at $\epsilon_{L\uparrow}$). This electron tunnels to the right dot absorbing $k_1 - k$ photons and goes back to the left dot emitting $n - k$ photons. Then this electron has energy $\epsilon_{L\uparrow} + (k_1 - n)\hbar\omega$, which has a difference $(k_1 - n)\hbar\omega$ from the resonance state $\epsilon_{L\uparrow}$, and there is no state at energy $\epsilon_{L\uparrow} + (k_1 - n)\hbar\omega$. Therefore this processes ($k_1 \neq n$) has very small probability to occur. In fact, when ϵ is near a resonant state (*e.g.* $\epsilon_{L\uparrow}$), $g_{\alpha\alpha\sigma}^r(\epsilon)$ [Eq.(3) in the manuscript] can be rewritten as $1/(\epsilon - \epsilon_{L\uparrow} + i\delta)$. Then the term in the left side of Eq.(C6) can be rewritten as:

$$\frac{A_{R\sigma,k_1n}}{(\epsilon - \epsilon_{L\uparrow} + k_1\hbar\omega + i\delta)(\epsilon - \epsilon_{L\uparrow} + n\hbar\omega + i\delta)} \quad (C7)$$

where δ is a small positive real number ($\sim \Gamma$). Now it clearly shows that when $k_1 \neq n$, this term is always very small for any electron energy ϵ [note that $A_{R\sigma,k_1n}$ has a small factor t_C^2]. When $k_1 = n$, this term is large at $\epsilon = \epsilon_{L\uparrow} - n\hbar\omega$. Therefore our approximation is reasonable if $\hbar\omega \gg \max(\Gamma_\alpha, t_C)$.

Under this approximation, we can easily solve $G_{LL\sigma,mn}^r$ from Eq.(C5)

$$G_{LL\sigma,mn}^r(\epsilon) = \frac{\delta_{mn}}{\left(g_{LL\sigma,mm}^r\right)^{-1} - A_{R\sigma,mm}} \quad (C8)$$

Then, $G_{LR\sigma,mn}^r$ can be obtained immediately:

$$G_{LR\sigma,mn}^r(\epsilon) = G_{LL\sigma,mm}^r(\epsilon)\Sigma_{LR\sigma,mn}^r g_{RR\sigma,nn}^r(\epsilon) \quad (C9)$$

$G_{RR\sigma,mn}^r(\epsilon)$ and $G_{RL\sigma,mn}^r(\epsilon)$ can also be solved in the same manner.

REFERENCES

- [1] S.A. Wolf, *et al*, Science **294**, 1488 (2001).
- [2] G.A. Prinz, Science **282**, 1660 (1998).
- [3] There have been some work on spin current generation by a rotating magnetic field in a *uni-pole* device. A uni-pole system, however, cannot function as a spin-cell because it cannot complete a spin-circuit. See, A. Brataas, Y. Tserkovnyak, G.E.W. Bauer, and B. Halperin, Phys. Rev. B **66**, 060404 (2002); B. Wang, J. Wang, and H. Guo, cond-mat/0208475 (2002).
- [4] A.-P. Jauho, N.S. Wingreen, and Y. Meir, Phys. Rev. B **50**, 5528 (1994).
- [5] T.H. Oosterkamp, *et al*, Nature **395**, 873 (1998).
- [6] N.S. Wingreen, A.-P. Jauho, and Y. Meir, Phys. Rev. B, **48**,8487 (1993).
- [7] In deriving the (nonperturbed) retarded Green's function of H_o , we have taken a decoupling approximation as:
- $$\begin{aligned} \ll a_{\alpha k \sigma} d_{\alpha \bar{\sigma}}^\dagger d_{\alpha \bar{\sigma}} | d_{\alpha \sigma}^\dagger \gg^r &= n_{\alpha \bar{\sigma}} \ll a_{\alpha k \sigma} | d_{\alpha \sigma}^\dagger \gg^r, \\ \ll a_{\alpha k \bar{\sigma}}^\dagger d_{\alpha \sigma} d_{\alpha \bar{\sigma}} | d_{\alpha \sigma}^\dagger \gg^r &= \ll a_{\alpha k \bar{\sigma}}^\dagger d_{\alpha \bar{\sigma}}^\dagger d_{\alpha \sigma} | d_{\alpha \sigma}^\dagger \gg^r = 0. \end{aligned}$$
- In this approximation the level renormalization has been neglected. Because our system is in the Coulomb blockade regime, the level renormalization is very small and this approximation is reasonable. Even if the level renormalization is included, it does not affect the working principle of the spin-cell.
- [8] Q.-f. Sun, J. Wang, and T.-h. Lin, Phys. Rev. B **59**, 13126 (1999).
- [9] Because H_0 has interaction U_α , this Dyson equation is not exact, but is a good approximation.
- [10] Here we took the same approximation as that of Ref. [8] which is reasonable when $\hbar\omega \gg \max(\Gamma_\alpha, t_C)$.

- [11] If resistances of the external circuit for spin-up and spin-down channels are slightly different, the spin-cell will drive a large spin current perhaps with a small charge current. However, by regulating the gate voltage V_g which makes the spin-motive force also slightly different for spin-up and spin-down electrons, we can still obtain a spin-current with zero charge-current.
- [12] The frequency ω^* of the spin-cell operation point A (see Fig.(1c)) actually depends on the value of B_L : $2\hbar\omega^* = \epsilon_{L\downarrow} + U_L + \epsilon_{R\uparrow} + U_R - \epsilon_{L\uparrow} - \epsilon_{R\downarrow} = U_L + U_R + g\mu(B_L - B_R)$. To plot Fig.(3b) we varied ω^* for each value of B_L accordingly.
- [13] T.H. Oosterkamp, *et al*, Phys. Rev. Lett. **78**, 1536 (1997).
- [14] L.P. Kouwenhoven, *et al*, Phys. Rev. Lett. **73**, 3443 (1994).
- [15] In order to calibrate experimental conditions at the spin-cell operating point, one needs a method to detect spin current outside the spin-cell. Recently, Hirsch has advanced a theoretical idea for this purpose which works even in the absence of a charge current: J.E. Hirsch, Phys. Rev. Lett. **83**, 1834 (1999). Moreover, the detection can be made easier if we allow and then detect a small charge current that flows through the spin-cell, using the two panels of Fig.(2) as a “map” between the charge and spin currents.

FIGURES

FIG. 1. (a). Schematic diagram for a conductor which has a spin current with zero charge current; (b). Schematic diagram for the double quantum dot spin-cell; (c). Schematic plot for the spin-cell operation via photon-assisted tunneling processes indicated by $A\pm$.

FIG. 2. The charge current I_e and spin current I_s versus gate voltage V_{gR} for different frequencies ω . Different curves have been offset such that the vertical axis gives the frequency. Two dotted oblique lines $A\pm$ indicate the position of the peaks. The parameters are: $\mu_L = \mu_R = 0$, $\Gamma_L = \Gamma_R = k_B T = 0.1$, $t_C = 0.02$, $U_L = 1$, $U_R = 0.9$, $g\mu B_L = 0.2$, $g\mu B_R = -0.4$, $V_{gL} = 0.5$, $V_g = 0$, and $\Delta/\omega = 1.0$.

FIG. 3. (a), (b), and (c) are I_e and I_s versus gate voltage V_g , the magnetic field $g\mu B_L$, and frequency ω , respectively. $\omega = 1.25$ in (a); $2\omega = U_L + U_R + g\mu(B_L - B_R)$ in (b). $V_{gR} = 0.45$, and other parameters are the same as Fig.2. The solid, dotted, and dashed lines correspond to $\Delta/\omega = 2.0$, 1.0, and 0.5, respectively. Notice that the three curves of charge current overlap and they are all essentially zero.

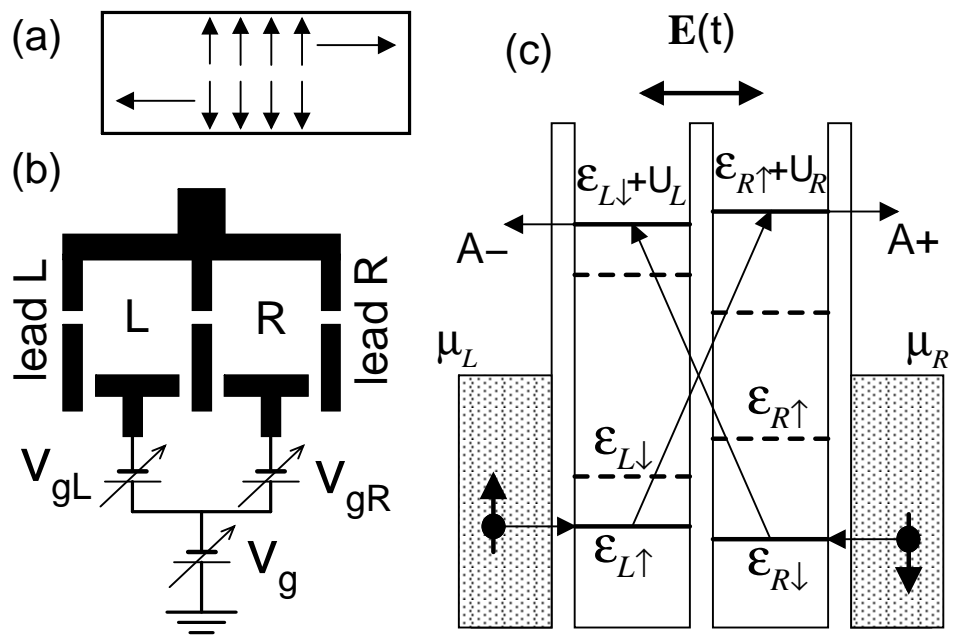


Fig.1

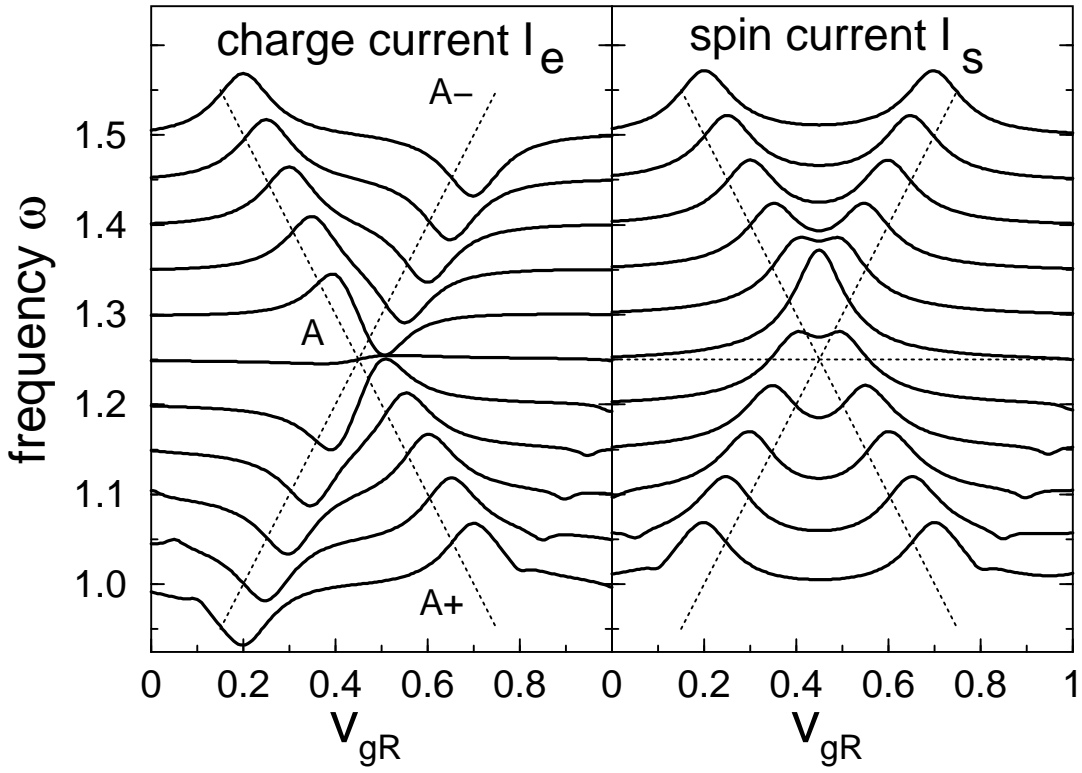


Fig.2

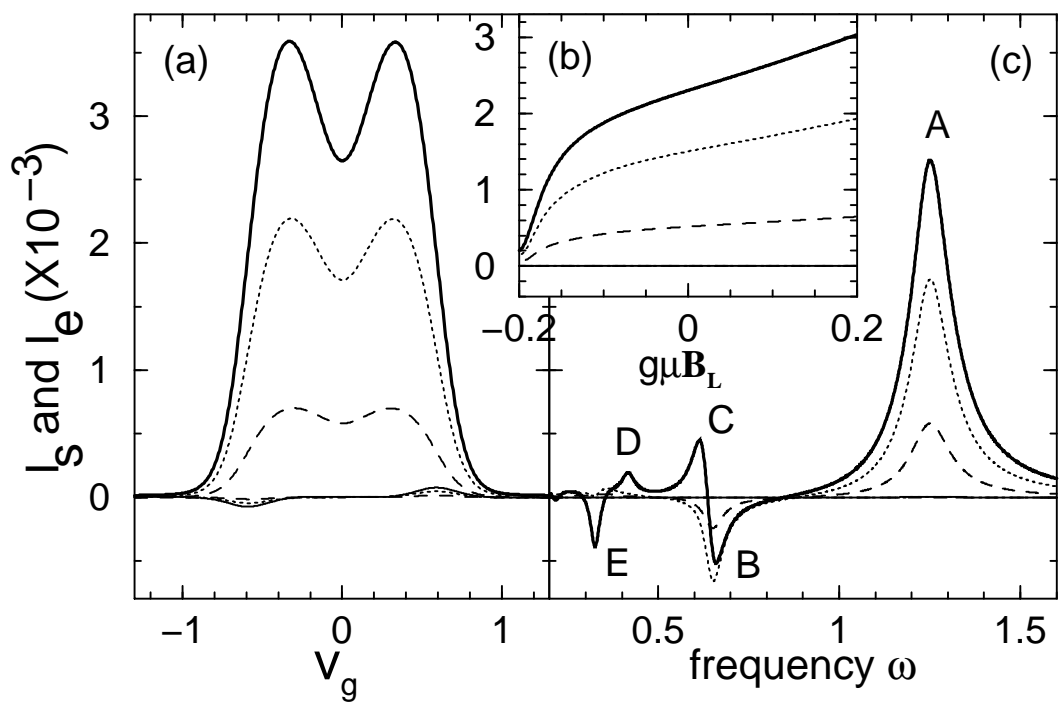


Fig.3